

# Estimating density and magnetic field turbulence in solar flares using radio zebra observations

M. Karlický<sup>1</sup> and L. Yasnov<sup>2,3</sup>

<sup>1</sup> Astronomical Institute of the Czech Academy of Sciences, Fričova 298, 251 65 Ondřejov, Czech Republic  
e-mail: karlicky@asu.cas.cz

<sup>2</sup> St.-Petersburg State University, 198504 St.-Petersburg, Russia

<sup>3</sup> St.-Petersburg Branch of Special Astrophysical Observatory, 196140 St.-Petersburg, Russia

Received 12 March 2020 / Accepted 10 April 2020

## ABSTRACT

**Context.** In solar flares the presence of magnetohydrodynamic turbulence is highly probable. However, information about this turbulence, especially the magnetic field turbulence, is still very limited.

**Aims.** In this paper we present a new method for estimating levels of the density and magnetic field turbulence in time and space during solar flares at positions of radio zebra sources.

**Methods.** First, considering the double-plasma resonance model of zebras, we describe a new method for determining the gyro-harmonic numbers of zebra stripes based on the assumption that the ratio  $R = L_b/L_n$  ( $L_n$  and  $L_b$  are the density and magnetic field scales) is constant in the whole zebra source.

**Results.** Applying both the method proposed in this work and one from a previous paper for comparison, in the 14 February 1999 zebra event we determined the gyro-harmonic numbers of zebra stripes. Then, using the zebra-stripe frequencies with these gyro-harmonic numbers, we estimated the density and magnetic field in the zebra-stripe sources as  $n = (2.95-4.35) \times 10^{10} \text{ cm}^{-3}$  and  $B = 17.2-31.9 \text{ G}$ , respectively. Subsequently, assuming that the time variation of the zebra-stripe frequencies is caused by the plasma turbulence, we determined the level of the time varying density and magnetic field turbulence in zebra-stripe sources as  $|\Delta n/n|_t = 0.0112-0.0149$  and  $|\Delta B/B|_t = 0.0056-0.0074$ , respectively. The new method also shows deviations in the observed zebra-stripe frequencies from those in the model. We interpret these deviations as being caused by the spatially varying turbulence among zebra-stripe sources; i.e., they depend on their gyro-harmonic numbers. Comparing the observed and model zebra-stripe frequencies at a given time, we estimated the level of this turbulence in the density and magnetic field as  $|\Delta n/n|_s = 0.0047$  and  $|\Delta B/B|_s = 0.0024$ . We found that the turbulence levels depending on time and space in the 14 February 1999 zebra event are different. This indicates some anisotropy of the turbulence, probably caused by the magnetic field structure in the zebra source.

**Key words.** Sun: flares – Sun: radio radiation – turbulence

## 1. Introduction

Solar flares are characterized by fast plasma flows, e.g., by plasma outflows from the magnetic reconnection (Priest & Forbes 2000). If in such plasma flows there are sufficiently strong shears in flow velocities, then owing to the Kelvin–Helmholtz (shear flow) instability, magnetohydrodynamic turbulence is generated (Chiueh & Zweibel 1987). This turbulence plays an important role in particle acceleration (Miller et al. 1996; Petrosian 2016). Some estimations of the level of this turbulence were made based on the broadening of the observed spectral lines (Hassler et al. 1990; Harra et al. 2013; Polito et al. 2018). In the paper by Karlický (2014) the frequency variations of the zebra stripes were interpreted as being caused by the plasma turbulence. These frequency variations were analyzed by the Fourier method and the spectra with the power-law index close to the Kolmogorov index were found.

In the present paper we estimate the levels of the time and spatially varying turbulence in the density and magnetic field in the zebra radio sources observed during solar flares. In particular, the estimation of the levels of the magnetic field turbulence is new.

We use the zebra model based on the double-plasma resonance (DPR) instability (Zheleznyakov & Zlotnik 1975; Winglee & Dulk 1986; Kuznetsov & Tsap 2007; Tan 2010; Zlotnik 2013; Tan et al. 2014; Karlický & Yasnov 2015; Benáček & Karlický 2019). In this model, each zebra-stripe source is located at a different place. It enables us to estimate the turbulence level not only in each zebra-stripe source (time varying turbulence), but also the turbulence level in space between the zebra-stripe sources at a given time (spatially varying turbulence).

The spatially varying turbulence between zebra-stripe sources is a new aspect in the zebra-stripe analysis. Moreover, it removes some problems with the DPR zebra model recently discussed in the paper by Yasnov & Chernov (2020). The authors calculated a sequence of the gyro-harmonic numbers of zebra stripes in the whole zebra from the zebra-stripe frequencies at the high- and low-frequency parts of the zebras. They found that the sequence of the gyro-harmonic numbers derived from the high- and low-frequency zebra stripes differ in some zebras. Based on this, they concluded that these zebras cannot be explained by the DPR model. However, when we include the turbulence in the DPR model then the difference in calculated sequences of the gyro-harmonic numbers can be explained within the DPR

model. In the DPR model the zebra-stripe sources are located at different positions, and thus the plasma turbulence modifies the zebra-stripe frequencies of different zebra stripes in a different way. This introduces a difference in the sequence of the gyro-harmonic numbers calculated from the high- and low-frequency parts of the zebras.

In this paper we also present a new method for determining the gyro-harmonic numbers of the zebra stripes. The results obtained by this new method are verified by our previous method, presented in the paper by [Karlický & Yasnov \(2015\)](#). We apply these methods for the 14 February 1999 zebra event and calculate not only the gyro-harmonic numbers of zebra stripes, but also the density and magnetic field. Then, knowing the gyro-harmonic numbers of zebra stripes in this zebra event, we estimate the level of the time varying and spatially varying turbulence in the density and magnetic field in the zebra-stripe sources. This enables us to compare these turbulence levels for the first time.

## 2. Method and its application

In our method we use the zebra model based on the double-plasma resonance (DPR) instability ([Zheleznyakov & Zlotnik 1975](#); [Winglee & Dulk 1986](#); [Zlotnik 2013](#); [Benáček & Karlický 2018](#)). Our method consists of two steps. First, we determine the gyro-harmonic numbers of zebra stripes by a new method and by our previous methods ([Karlický & Yasnov 2015](#)). Second, knowing the gyro-harmonic numbers and the zebra-stripe frequencies, we calculate the density and magnetic field in the zebra-stripe sources, and also their temporal and spatial variations, and thus the levels of their turbulence. The new method for determining the gyro-harmonic numbers is highlighted by the example below where we use artificially generated zebra-stripe frequencies. Then this new method is applied to the observed zebra.

In the DPR model the ratio of the two different zebra-stripe frequencies can be expressed as ([Karlický & Yasnov 2019](#))

$$\frac{f^{s+m}}{f^s} = \frac{s+m}{s} \left( \frac{(s+m)^2 - 1}{s^2 - 1} \right)^{\frac{1}{R-2}}, \quad (1)$$

where  $f_s$  and  $f_{s+m}$  are the zebra-stripe frequencies for the zebra stripe with the gyro-harmonic numbers  $s$  and  $s+m$ ;  $R = L_b/L_n$ , where  $L_n$  and  $L_b$  is the density and magnetic field scale in the density  $n$  and magnetic field  $B$  profiles

$$n = n_0 \exp^{-\frac{h}{L_n}}, B = B_0 \exp^{-\frac{h}{L_b}}, \quad (2)$$

assumed in the zebra source;  $n_0$  and  $B_0$  are the density and magnetic field at some reference level; and  $h$  means the distance along the axis of the source.

In order to highlight our new method for determining the gyro-harmonic numbers of zebra stripes, we employ model (artificial) zebra-stripe frequencies. We use relation (1) with  $R = 0.65$ , which corresponds to sequence A ([Karlický & Yasnov 2018](#)); i.e., the zebra-stripe frequency in the zebra increases with decreasing gyro-harmonic number. We take this sequence A because it agrees with all zebras analyzed so far. We define the gyro-harmonic number  $s_L$  for the lowest zebra-stripe frequency  $f_L$ . In our example, we take  $s_L = 30$  for  $f_L = 1250$  MHz. In the relation (1) we change  $m$  from  $-1$  to  $-6$ , and calculate seven model zebra-stripe frequencies ( $F_{\text{model}} = 1250, 1270, 1292, 1315, 1339, 1365, \text{ and } 1392$  MHz).

Solving Eq. (1) for  $R$  we express  $R$  as  $R_{1,2}$  (i.e., in terms of the ratio of neighboring zebra-stripe frequencies and corresponding gyro-harmonic numbers). Thus, we obtain the relation as

$$R_{1,2} = 2 + \frac{\log\left(\frac{s_2^2 - 1}{s_1^2 - 1}\right)}{\log\left(\frac{s_1 f_1^{s_2}}{s_2 f_1^{s_1}}\right)}. \quad (3)$$

Here  $R_{1,2}$  is computed between the zebra-stripe frequency 1 and higher neighboring zebra-stripe frequency 2, starting from the lowest frequency  $f_L$ . In the following we make a number of computations of  $R_{1,2}$  for all pairs of neighboring zebra-stripe frequencies using the  $s_L$  as free parameter. We calculated  $R_{1,2}$  for the  $F_{\text{model}}$  frequencies and for six values of  $s_L = 15, 20, 25, 30, 35, \text{ and } 40$ .

In Fig. 1 we present the plots of these  $R_{1,2}$  values in dependence on the gyro-harmonic number  $s$ , including the regression lines. The red asterisks with the horizontal regression line in Fig. 1 correspond to the plot with  $s_L = 30$ . As expected in this case, in all computed pairs of frequencies  $R_{1,2}$  is equal to 0.65, as in the case when the model zebra-stripe frequencies were calculated from the relation (1) with  $s_L = 30$  and  $R = 0.65$ . But, when we use a value of  $s_L$  lower than 30 to calculate  $R_{1,2}$ , then the value of  $R_{1,2}$  increases with increasing  $s$ . On the other hand, when we use a value of  $s_L$  greater than 30 to calculate  $R_{1,2}$ , then the value of  $R_{1,2}$  decreases with increasing  $s$  (see Fig. 1). It should be noted that we fitted all the plots of  $R_{1,2}$  by the straight line – regression line. Except the case with  $s_L = 30$ , where  $R_{1,2}$  lie on the regression line, the other plots of  $R_{1,2}$  subtly deviate from the regression lines and the deviations increase with increasing  $|s_L - 30|$ . In the following, we utilize the change in the slope of the  $R_{1,2}$  plots shown in Fig. 1 to calculate  $s_L$  and  $R$  in the observed zebra. The actual value of  $s_L$  is determined when the regression line in the  $R_{1,2}$  data, calculated from the observed zebra-stripe frequencies, has a minimum slope compared to the horizontal line. This solution also gives the value of  $R = \text{constant}$ .

For a calculation based on observations, we use the zebra recorded on 14 February 1999 by the Ondřejov radiospectrograph ([Jiříčka et al. 1993](#)) (Fig. 2). As seen in this figure, the most distinct and continuous zebra stripes appear at approximately 12:08:57.0 UT. The zebra-stripe frequencies at this time are 1548, 1573, 1599, 1619, 1642, 1674, 1707, 1739, 1770, 1810, 1845, and 1880 MHz. We use these frequencies to determine the gyro-frequency numbers. We vary  $s_L$  in a reasonable interval from 10 to 70, and calculate plots of  $R_{1,2}$ . For each  $R_{1,2}$  plot we compute the regression line in the same way as the variation in the slope of the  $R_{1,2}$  plots in Fig. 1, looking for such  $s_L$  that the regression line has a minimum slope (i.e., this regression line represents  $R = \text{constant}$ ). In Fig. 3b we show  $R_{1,2}$  for the 14 February 1999 zebra versus  $s$  in the case when the regression line has the minimum slope. In this case  $s_L = 32$  and the  $R$  corresponding to the regression (dashed) line is 0.625. For comparison, Figs. 3a and c show cases for  $s_L = 22$  and  $s_L = 42$ ; we see in this case that the slope of the regression lines change with  $s_L$ , exactly like those in Fig. 1.

We checked the resulting  $s_L$  and  $R$  using our previous method, which is described in [Karlický & Yasnov \(2015\)](#). The results from this previous method are the same ( $s_L = 32$  and  $R = 0.625$ ).

Now, knowing the gyro-harmonic numbers of the zebra stripes and using the relations

$$n[\text{cm}^{-3}] = \frac{f_s^2(1 - 1/s^2)}{8.1 \times 10^{-5}}, B[G] = \frac{f_s}{2.8 s}, \quad (4)$$

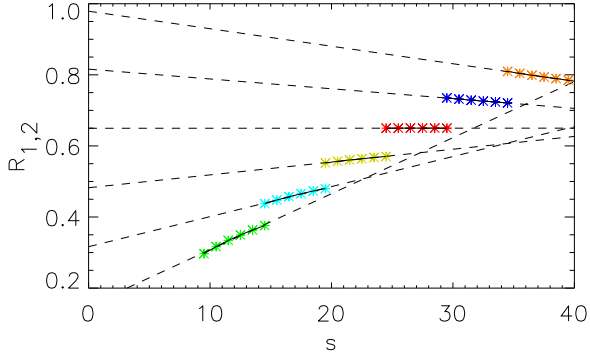


**Fig. 1.** Ratio of  $R_{1,2}$  in dependence on the gyro-harmonic number  $s$  for six values of  $s_L = 15$  (green asterisks), 20 (light blue), 25 (yellow), 30 (red), 35 (dark blue), and 40 (orange). Dashed lines mean the regression lines for all  $R_{1,2}$ .

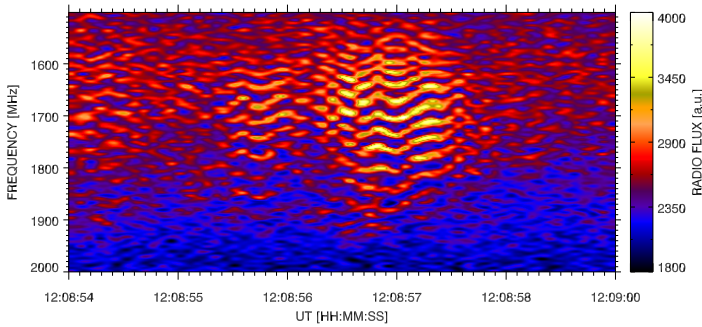


**Fig. 2.** Radio spectrum showing the zebra observed at 14 February 1999.

where  $f_s$  is in MHz, we calculated the density  $n$  and magnetic field  $B$  in the zebra-stripe sources at 12:08:57.0 UT. The results for each zebra-stripe source, designated by  $s$ , are in Table 1.

Now, let us estimate the level of turbulence in the zebra source. First, we estimate the level of the time varying turbulence. For this purpose we take the zebra-stripe frequencies at eight zebra stripes in the eight equal consecutive windows covering the interval 12:08:56.7–12:08:57.4 UT, i.e., at a time around 12:08:57.0 UT where the gyro-harmonic numbers were determined and where there are continuous zebra stripes. Using the relations in Eq. (4) we calculated the variations in density and magnetic field in the zebra-stripe sources in comparison to their mean values. The results are shown in Fig. 4. The level of the time varying turbulence in density and magnetic field, expressed as the standard deviation for each window, is  $|\Delta n/n|_t = 0.0112$ – $0.0149$  and  $|\Delta B/B|_t = 0.0056$ – $0.0074$ .

Now, let us estimate the level of the spatially varying turbulence. Figure 3b shows that  $R_{1,2}$  varies, which means that the observed zebra-stripe frequencies differ from those in the model, where  $R = 0.625$  (dashed line). Although the error in zebra-stripe frequency measurements, which is  $\sim 2$  MHz, can contribute to this variation, we assume that the variation is caused by the plasma turbulence in the zebra-stripe sources.

Using the lowest zebra-stripe frequency in the 14 February 1999 zebra ( $f_L = 1548$  MHz) and computed values of  $s_L = 32$  and  $R = 0.625$  we generate the model frequencies according to relation (1). Thus, for all zebra stripes with  $s$  we know the observed and model frequencies. Using these frequencies and the relations in Eq. (4), we compute the frequency difference between the observed and modeled frequencies  $\Delta f$  and the variation in the density  $\Delta n/n$  and magnetic field  $\Delta B/B$  in all zebra-stripe sources. The results are shown in Fig. 5. The corresponding

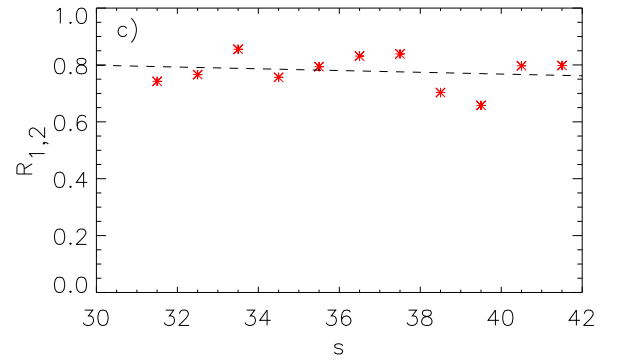
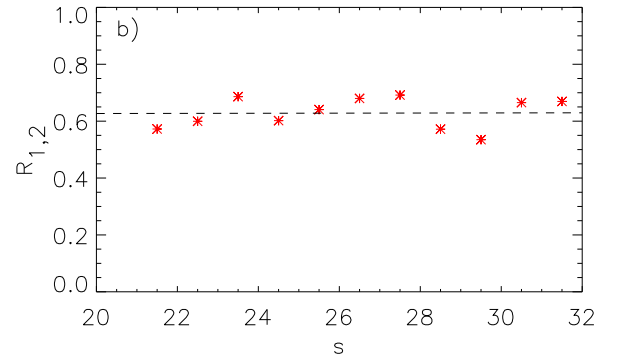
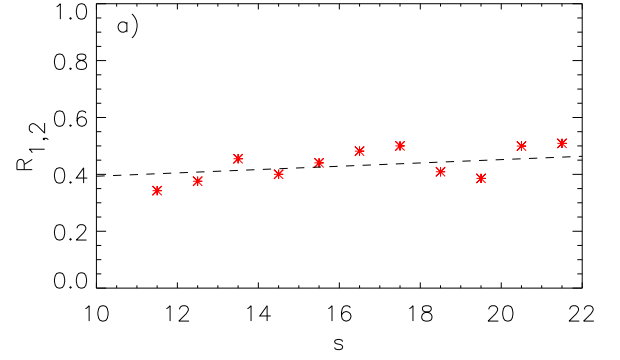


**Fig. 3.**  $R_{1,2}$  in dependence on  $s$ , derived from the 14 February 1999 zebra: (a) for  $s_L = 22$ , (b) for  $s_L = 32$ , and (c) for  $s_L = 42$ . Dashed lines mean the regression lines. In case (b) the regression line has a minimum slope compared to the horizontal line. Thus, this case gives the resulting  $s_L = 32$  and  $R = 0.625$ .

levels of the spatially varying turbulence expressed as the standard deviations are  $|\Delta n/n|_s = 0.0047$  and  $|\Delta B/B|_s = 0.0024$ .

### 3. Discussion and conclusions

In this paper we presented not only a new method for estimating the plasma turbulence level in the zebra-stripe radio sources, but also a new method for determining the gyro-harmonic numbers  $s$  in zebras. The method used to determine  $s$  is equivalent to the method presented in Karlický & Yasnov (2015).

We estimated levels of the time and spatially varying turbulence in the zebra stripe sources. The estimated levels are  $|\Delta n/n|_t = 0.0112$ – $0.0149$  and  $|\Delta B/B|_t = 0.0056$ – $0.0074$  for the time varying turbulence and  $|\Delta n/n|_s = 0.0047$  and  $|\Delta B/B|_s = 0.0024$  for the spatially varying turbulence. These turbulence levels differ in that the level of the spatially varying

**Table 1.** Density and magnetic field in the zebra-stripe sources at 12:08:57.0 UT in the 14 February 1999 zebra.

$f$ (MHz)	1548	1573	1599	1619	1642	1674	1707	1739	1770	1810	1845	1880
$s$	32	31	30	29	28	27	26	25	24	23	22	21
$n$ ( $10^{10} \text{ cm}^{-3}$ )	2.95	3.05	3.15	3.23	3.32	3.45	3.59	3.72	3.86	4.03	4.19	4.35
$B$ (G)	17.2	18.1	19.0	19.9	20.9	22.1	23.4	24.8	26.3	28.1	29.9	31.9

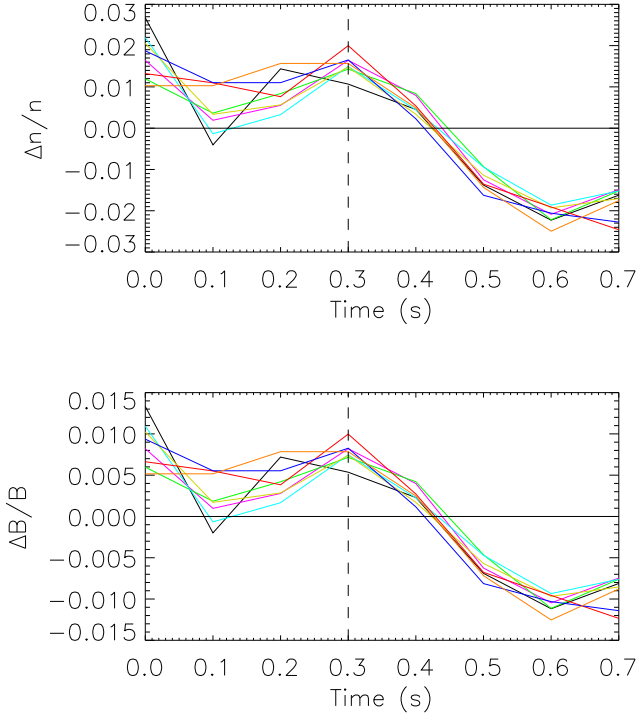


**Fig. 4.** Time variations of the density  $\Delta n/n$  and magnetic field  $\Delta B/B$  in the time interval 12:08:56.7–12:08:57.4 UT for the 14 February 1999 zebra. Black line:  $s = 28$ ; violet:  $s = 27$ ; green:  $s = 26$ ; light blue:  $s = 25$ ; yellow:  $s = 24$ ; red:  $s = 23$ ; blue:  $s = 22$ ; and orange:  $s = 21$ . The vertical dashed line shows the time 12:08:57 UT, when the calculation of the gyro-harmonic numbers was made.

turbulence is lower. It indicates some anisotropy of this turbulence, probably caused by the magnetic field structure around zebra-stripe sources.

As seen in Figs. 4 and 5, variations in the density and magnetic field are in phase, which indicates the fast magnetosonic wave turbulence. The estimated turbulence levels are partly corrupted by the errors on the observed zebra-stripe frequencies. The estimated error on this determination is about 2 MHz, to be compared with the maximum difference between the zebra-stripe frequency and the mean zebra-stripe frequency in the studied interval (12:08:56.7–12:08:57.4 UT) ( $\sim 20$  MHz), and the maximum difference between model and observed zebra-stripe frequencies ( $\sim 10$  MHz; Fig. 5).

Figure 6 shows the regions of the plasma beta parameter greater or smaller than 1 in dependence on the plasma temperature and the gyro-harmonic number  $s$  of zebra stripes. This plot is made using the plasma beta definition and the relations in Eq. (4). As seen in this figure, the plasma beta parameter in the zebra-stripe sources is lower than 1 if the temperature is at least 1 MK (coronal temperature) and the gyro-harmonic numbers is smaller than about 50. For higher gyro-harmonic numbers and  $\beta \leq 1$ , the temperature in the zebra-stripe sources is

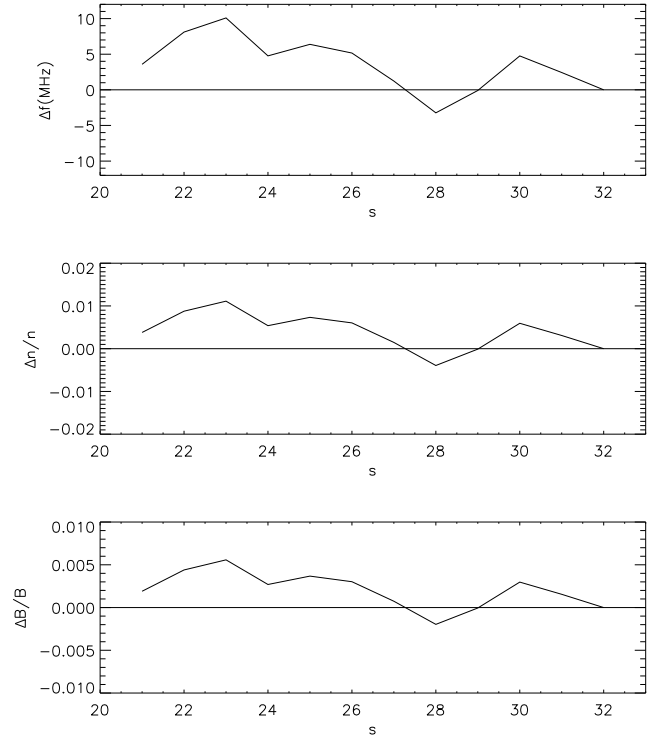


**Fig. 5.** Frequency difference between the observed and modeled zebra-stripe frequencies  $\Delta f$ , and variations in the density  $\Delta n/n$  and magnetic field  $\Delta B/B$  in dependence on the gyro-harmonic number  $s$  at 12:08:57 UT for the 14 February 1999 zebra.

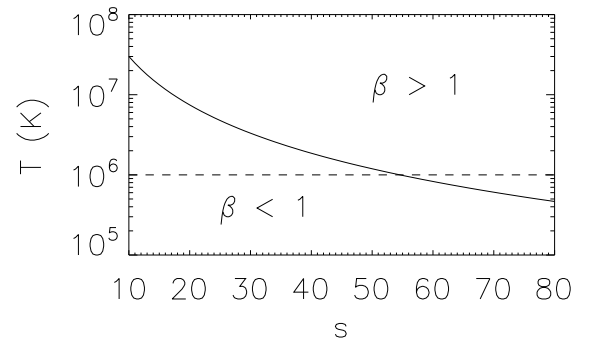


**Fig. 6.** Regions of the plasma beta parameter  $\beta > 1$  and  $\beta < 1$  in the diagram of the plasma temperature vs. the gyro-harmonic number  $s$ .

lower than 1 MK. In our case of the 14 February 1999 zebra, the gyro-harmonic number  $s_L$  is 32; therefore, the temperature in the zebra source for the plasma beta parameter  $\beta < 1$  can be up to 3 MK.

*Acknowledgements.* The authors thank the referee for constructive comments that improved the article. We acknowledge support from the project RVO-67985815 and GACR grants 18-09072S, 19-09489S, 20-09922J, and

20-07908S. L. V. Yasnov acknowledges support from the Russian Foundation for Basic Research, Grants 18-29-21016-mk, and partly from Grant 18-02-00045, from Program RAN No.28, Project 1D and State Task No. AAAA-A17-117011810013-4.

## References

- Benáček, J., & Karlický, M. 2018, *A&A*, **611**, A60  
Benáček, J., & Karlický, M. 2019, *ApJ*, **881**, 21  
Chiueh, T., & Zweibel, E. G. 1987, *ApJ*, **317**, 900  
Harra, L. K., Matthews, S., Culhane, J. L., et al. 2013, *ApJ*, **774**, 122  
Hassler, D. M., Rottman, G. J., Shoub, E. C., & Holzer, T. E. 1990, *ApJ*, **348**, L77  
Jiříčka, K., Karlický, M., Kepka, O., & Tlamicha, A. 1993, *Sol. Phys.*, **147**, 203  
Karlický, M. 2014, *A&A*, **561**, A34  
Karlický, M., & Yasnov, L. V. 2015, *A&A*, **581**, A115  
Karlický, M., & Yasnov, L. V. 2018, *ApJ*, **867**, 28  
Karlický, M., & Yasnov, L. 2019, *A&A*, **624**, A119  
Kuznetsov, A. A., & Tsap, Y. T. 2007, *Sol. Phys.*, **241**, 127  
Miller, J. A., Larosa, T. N., & Moore, R. L. 1996, *ApJ*, **461**, 445  
Petrosian, V. 2016, *ApJ*, **830**, 28  
Polito, V., Dudík, J., Kašparová, J., et al. 2018, *ApJ*, **864**, 63  
Priest, E., & Forbes, T. 2000, *Magnetic Reconnection* (Cambridge, UK: Cambridge University Press)  
Tan, B. 2010, *Astrophys. Space Sci.*, **325**, 251  
Tan, B., Tan, C., Zhang, Y., et al. 2014, *ApJ*, **790**, 151  
Winglee, R. M., & Dulk, G. A. 1986, *ApJ*, **307**, 808  
Yasnov, L. V., & Chernov, G. P. 2020, *Sol. Phys.*, **295**, 13  
Zheleznyakov, V. V., & Zlotnik, E. Y. 1975, *Sol. Phys.*, **44**, 461  
Zlotnik, E. Y. 2013, *Sol. Phys.*, **284**, 579